

## Accepted Manuscript

Restraining fluoride loss from NaYF<sub>4</sub>:Yb<sup>3+</sup>,Er<sup>3+</sup> upconverting nanoparticles in aqueous environments using crosslinked poly(acrylic acid)/poly(allylamine hydrochloride) multilayers

Emilia Palo, Mikko Salomäki, Mika Lastusaari

PII: S0021-9797(18)31418-8  
DOI: <https://doi.org/10.1016/j.jcis.2018.11.094>  
Reference: YJCIS 24359

To appear in: *Journal of Colloid and Interface Science*

Received Date: 8 October 2018  
Revised Date: 22 November 2018  
Accepted Date: 24 November 2018

Please cite this article as: E. Palo, M. Salomäki, M. Lastusaari, Restraining fluoride loss from NaYF<sub>4</sub>:Yb<sup>3+</sup>,Er<sup>3+</sup> upconverting nanoparticles in aqueous environments using crosslinked poly(acrylic acid)/poly(allylamine hydrochloride) multilayers, *Journal of Colloid and Interface Science* (2018), doi: <https://doi.org/10.1016/j.jcis.2018.11.094>

This is a PDF file of an unedited manuscript that has been accepted for publication. As a service to our customers we are providing this early version of the manuscript. The manuscript will undergo copyediting, typesetting, and review of the resulting proof before it is published in its final form. Please note that during the production process errors may be discovered which could affect the content, and all legal disclaimers that apply to the journal pertain.



Restraining fluoride loss from  $\text{NaYF}_4:\text{Yb}^{3+},\text{Er}^{3+}$   
upconverting nanoparticles in aqueous environments  
using crosslinked poly(acrylic acid)/poly(allylamine  
hydrochloride) multilayers

*Emilia Palo*\*<sup>a,b</sup>, *Mikko Salomäki*<sup>a,c</sup>, and *Mika Lastusaari*<sup>a,c</sup>

<sup>a</sup> University of Turku, Department of Chemistry, FI-20014 Turku, Finland

<sup>b</sup> University of Turku Graduate School (UTUGS), Doctoral Programme in Physical and  
Chemical Sciences, Turku, Finland

<sup>c</sup> Turku University Centre for Materials and Surfaces (MatSurf), Turku, Finland

**Corresponding author**

\* emilia.palo@utu.fi

**KEYWORDS:** layer-by-layer; polyelectrolytes; crosslinking; nanoparticles; upconversion  
luminescence

## ABSTRACT

The use of upconverting nanoparticles in various applications in aqueous media relies on their surface modifications as most synthesis routes yield hydrophobic particles. However, introducing upconverting nanoparticles in aqueous solutions commonly results in the quenching of their luminescence intensity and in the worst case, disintegration of the nanoparticles. We demonstrate the use of poly(acrylic acid) and poly(allylamine hydrochloride) as a protecting layer-by-layer coating for the upconverting  $\text{NaYF}_4:\text{Yb}^{3+},\text{Er}^{3+}$  nanoparticles. The formation and crosslinking of the bilayer coating was confirmed with Fourier transform infrared spectroscopy, thermal analysis and zeta potential. The release of internal fluoride ions from the nanoparticle structure and subsequent particle disintegration was decelerated especially by crosslinking the bilayer coating on the surface. In addition, we studied the effect of the coating on the upconversion luminescence properties and learned that with additional fluoride ions present during the layer-by-layer assembly the most intense enhancement in the luminescent intensity is obtained. This is due both to not allowing the disintegration of the particles during the surface modification process as well as preventing the water molecules accessing the surface by crosslinking the bilayer coating.

## INTRODUCTION

The increasing research on the use of upconversion nanomaterials in various applications such as biosensors [1], biomedical assays and imaging [2,3] and in theranostics [4] is based on the materials' unique property of converting low energy radiation (mainly near infra-red, NIR) into higher energy radiation (visible light) [5,6]. The NIR excitation needed for upconversion nanomaterials provokes less photodamage in the imaged tissue in comparison with the

conventional ultraviolet (UV) excitation. Furthermore, the lack of autofluorescence in the background benefits especially the biomedical field enabling faster processes due to not needing time-resolved measurements [7]. While the development of smaller nanoparticles has widened their use range in research [8,9] there are drawbacks that need addressing. Hexagonal  $\beta$ -NaYF<sub>4</sub>:Yb<sup>3+</sup>,Er<sup>3+</sup> is probably the most widely used upconverting nanoparticle (UCNP) nowadays due to its superiority as the most efficient upconversion material [10,11]. However, one of the most crucial drawbacks in the NaYF<sub>4</sub> materials is the quenching of upconversion luminescence in aqueous environments through energy migration within the sensitizing ytterbium ions in the NaYF<sub>4</sub> lattice and the large surface area that can be full of impurities [12–14]. In addition to energy migration, recent studies suggest that this luminescence quenching is also caused by disintegration of the NaYF<sub>4</sub> UCNPs in aqueous media [15,16].

Methods of enhancing the performance of NaYF<sub>4</sub> UCNPs have been developed, such as manufacturing various types of core-shell materials [17,18] and using metal frameworks near the particle to induce plasmonic effects [19,20]. However, as long as the fluoride ions remain on the surface of the nanoparticle its disintegration is probable when the nanoparticles are in direct contact with water. Also, because most of the common synthesis methods produce hydrophobic nanoparticles [7,21], multiple surface functionalization steps need to be taken to enable the dispersion of the particles into water [2,22]. A few surface modification strategies for hindering the disintegration of UCNPs have already been published but none have been able to prevent the disintegration completely [23,24].

In the current study, we investigated the surface functionalization of UCNPs using a layer-by-layer method to produce bilayers with self-assembled negatively and positively charged polyelectrolytes, namely poly(acrylic acid) (PAA) and poly(allylamine hydrochloride) (PAH)

[25,26]. Nanoparticles have been used as a template for the layer-by-layer method previously when various types of bilayers have been manufactured [27–29]. However, the use of the layer-by-layer method in the surface functionalization of UCNPs has not been studied in detail as the bilayer formation is affected by a multitude of conditions during the process. Previously, it has been observed that by employing crosslinked PAA/PAH layers with a  $\text{Cu}^{2+}$ -template on a flat alumina surface it was possible to reduce the anion flux through the alumina membrane [30]. We wanted to investigate if cross-linking could be used to reduce or even prevent the outward fluoride flux from the  $\text{NaYF}_4$  particles that would cause the disintegration of UCNPs in aqueous environments.

The bilayer coating formation using PAA and PAH was studied with selected ionic concentrations at pH 5.5 which provides enough charge for both polyelectrolytes. Coating was also manufactured in the presence of an additional fluoride source to investigate the disintegration during the layer-by-layer coating cycles. Fourier transform infrared (FT-IR) spectroscopy, thermal analysis and zeta potential measurements were used to confirm the formed coating and the crosslinking of the bilayer structure. To see how the bilayers and their crosslinking affected the disintegration of the nanoparticles in aqueous environments the concentration of released internal fluoride was measured. Changes in the upconversion luminescence properties of the core materials was studied using a 973 nm excitation suitable for the excitation of  $\text{Yb}^{3+}$  and  $\text{Er}^{3+}$  ions.

## **MATERIALS AND METHODS**

### **Reagents.**

Poly(acrylic acid) (PAA;  $M_w \approx 100,000$ ),  $(C_3H_4O_2)_n$ , Aldrich), poly(allylamine hydrochloride) (PAH;  $M_w \approx 50,000$ ,  $[CH_2CH(CH_2NH_2 \cdot HCl)]_n$ , Aldrich), sodium chloride (NaCl 99.5 %, J.T. Baker), sodium fluoride (NaF, >99 % Fluka), sodium nitrate ( $NaNO_3$ , 99.5 % Riedel-de Haen). Absolute ethanol (>99.5 %, Altia) was used as received.

### Materials preparation.

The  $\beta$ - $NaYF_4:Yb^{3+},Er^{3+}$  ( $x_{Yb}$ : 0.17,  $x_{Er}$ : 0.03) nanoparticles (size *ca.* 19\*23 nm) used as the core material were prepared with the synthesis procedure reported previously [31]. The oleic acid present at the nanoparticle surface was removed with a previously described acidic treatment [32]. The coating solutions were 10 mM of used polyelectrolyte (in reference to the monomer concentration of the polyelectrolyte) solubilized in 0.1 or 0.2 M NaCl (aq). The pH of the solutions was 5.5. An additional layer-by-layer assembly using ionic concentration of 0.1 M NaCl was made with extra fluoride present. In this case an additional 10 mM of NaF was added into each used solution including the water used for washing.

The coating cycle of the nanoparticles was the same as reported previously [29]. The cycle involved dispersing the core nanoparticles into the desired coating solution and ultrasonicing for two minutes and washing with quartz distilled water twice to prepare half a bilayer. One, three and five bilayers were manufactured to ensure layer formation. Also an additional PAA layer was added on top with a similar procedure to provide attaching sites for biomolecules and to ensure suspension in water based solutions. This makes the total number of bilayers 1.5, 3.5 and 5.5. The crosslinking of the formed bilayers was performed at 180 °C (ramp step 2 °C/min) for two hours in a nitrogen atmosphere. The outermost layer of PAA was expected not to take

part in the crosslinking process to a great extent thus leaving negative carboxyl ends as attaching sites to the surface.

### Characterization

The core particles' crystal structure was determined at room temperature with X-ray powder diffraction (XRD) using a Huber G670 image plate Guinier camera (Cu  $K_{\alpha 1}$  radiation, 1.5406 Å) with a  $2\theta$  range of 4-100° (step 0.005°). Data collection time was 30 min followed by 10 data reading scans of the image plate. From this data the crystallite size of the core material was calculated with the Scherrer formula using reflections (002) and (200) for the thickness and width of the hexagonal faces, respectively.

The presence of the polyelectrolytes was studied with FT-IR spectra using Bruker Vertex 70 MVP Star Diamond setup with 256 scans between 450 and 4500  $\text{cm}^{-1}$ . The resolution was 4  $\text{cm}^{-1}$ .

The thermal behavior of the coated materials was studied with thermogravimetric analysis (TGA) and differential scanning calorimetry (DSC) using one measurement per sample with a TA Instruments SDT Q600 TGA-DSC apparatus. The measurements were made between 35 and 600 °C with the heating rate of 10 °C/min using flowing air sphere (100 ml/min). The error for weight is *ca.* 1 % in this setup. The Zeta potential of the materials was measured from three parallel measurements with Malvern Zetasizer Nano-ZS equipment. The concentration of aqueous solutions was 100  $\mu\text{g}/\text{ml}$  with pH of *ca.* 6. The images of the coated nanoparticles were obtained with JEM-1400 Plus transmission electron microscopy (TEM) using OSIS Quemesa 11 Mpix bottom mounted digital camera. The nanoparticles were suspended into ethanol and dried on a lacey carbon grid and then imaged with acceleration of 60 kV.

Disintegration of the nanoparticles was studied using fluoride selective electrode was studied with one measurement per sample. Known amount (*ca.* 2 mg) of the nanoparticles was combined with 1 ml of water and sealed in a dialysis tube (Orange Scientific, Regenerated cellulose dialysis tubing MWCO 3500). The dialysis tube with the contents was then immersed in aqueous solution of 0.1 M NaNO<sub>3</sub> (total volume 50 ml) with the ion selective and reference electrodes. The data was collected automatically once every minute during the 24 hour measurement window. When the measurements were made with external 10<sup>-5</sup> M NaF it was added into all solutions including the one inside the dialysis tube.

The upconversion luminescence spectra were measured at room temperature with an Avantes Avaspec HS-TEC spectrometer. A fiber-coupled continuous NIR laser diode IFC-975-008-F (Optical Fiber Systems) with the excitation wavelength of 973 nm (10 270 cm<sup>-1</sup>) was used as an excitation source with 5000 mA corresponding 9.1 Wcm<sup>-2</sup>. Dry nanomaterials were held inside a rotating capillary tube and measured with 20 averaging scans, 20 ms each. After the sample a short-pass filter with a cutoff of 750 nm (Newport) was used to exclude excitation radiation. The emission was collected at a 90° angle to the excitation and directed to the spectrometer with an optical fiber.

## RESULTS AND DISCUSSION

### Layer-by-layer assembly on the nanoparticles

The  $\beta$ -NaYF<sub>4</sub>:Yb<sup>3+</sup>,Er<sup>3+</sup> upconversion nanomaterials used as core materials in the layering process were of hexagonal form and *ca.* 19\*23 nm in size (Table S1). The removal of oleic acid surface was confirmed with the FT-IR measurements as the signals of the asymmetric and symmetric vibrations of COO<sup>-</sup> could be seen to decrease (Figure S1).

When the FT-IR spectra of the coated nanoparticles were measured it was observed that with all materials the characteristic vibrations from PAA and PAH electrolytes were present in the materials (Figure S2) [33,34]. This could be observed from the presence of asymmetric and symmetric vibrations from carboxyl groups  $\text{COO}^-$  (*ca.* 1400 and 1550  $\text{cm}^{-1}$ ) and  $\text{COOH}$  (1710  $\text{cm}^{-1}$ ) from PAA and a broader band from  $\text{NH}_2$  bending in PAH at 800-900  $\text{cm}^{-1}$ . The formation is considered to be similar to the bilayer formation between PAA and PAH established on a planar surface [30,33,35,36].

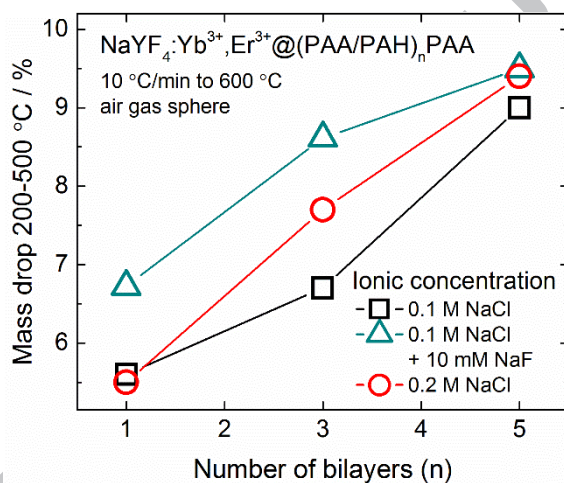


Figure 1. The mass drop of the coated UCNPs between 200 and 500 °C calculated from the thermal analysis data.

The thermal analysis of the coated nanoparticles suggested that the formation of bilayers varied between the deposition conditions (Figure 1, S3). It seemed that it is the most linear with the ionic concentration of 0.2 M. The percentage of the removed mass from the coated materials made with additional 10mM fluoride was higher from those prepared without fluoride. This suggested that in addition to interlocked water there were also residual fluoride ions from the additional fluoride solution in the bilayer structure that evaporates at higher temperatures

behaving similarly to amorphous NaF that is present in the annealing of cubic NaYF<sub>4</sub> structure [37]. However, the mass drop with five bilayers was similar in all of the coated materials and the difference in the behavior with the low number of bilayers is expected to arise only from the differences in the layer formation process. It could be that the higher ionic concentration is more efficient in stacking the polyelectrolyte to more compact and dense structures and thus making them easier to cover the nanoparticle surface without additional branched structures that might hinder uniform layer production and cause diversity into layers [38].

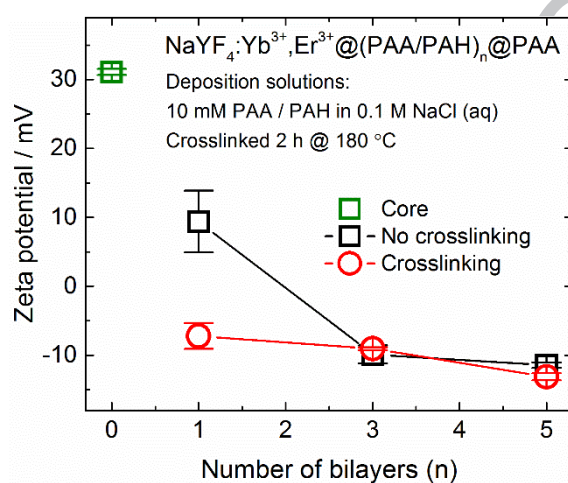


Figure 2. Zeta potential of the as-prepared and crosslinked coated nanomaterials prepared with ionic concentration of 0.1 M NaCl.

When zeta potential was considered, the nanomaterials regardless of the ionic concentrations during the layering process showed a similar trend in the surface behavior. The zeta potential changed from the core materials' *ca.* 30 mV to the *ca.* -10 mV of the materials having five bilayers (Figure 2, S4). Also the zeta potential of the materials deposited with additional 10 mM fluoride are similar to those deposited at the same conditions without the fluoride. This suggests that the amount of extra fluoride is low enough not to affect the bilayer formation. With all of the

coated nanomaterials the first bilayer showed the highest variation during measurement. This could indicate that the first bilayer structure is not as uniform as the following layers.

The TEM imaging of the coated nanoparticles was used to study if we observe the bilayer formation on the surface (Figure 3). As both polyelectrolytes used in the coating contain only very light elements in comparison with those in the  $\text{NaYF}_4:\text{Yb}^{3+},\text{Er}^{3+}$  core particles the imaging was made using a lacey carbon grid with low voltage (60 kV) to minimize the background and to give more contrast to the surface. Unfortunately the use of a carbon grid as a template aggregates the nanoparticles on the grid boundaries similarly as observed on the previous layer-by-layer coated nanoparticles [24,29]. While the exact amount of the bilayers cannot be seen from the TEM images, the coating was visible when the material coated with 5.5 bilayers of (PAA/PAH) was imaged. The thickness of the coating is *ca.* 2 nm which is similar to those obtained previously [29].

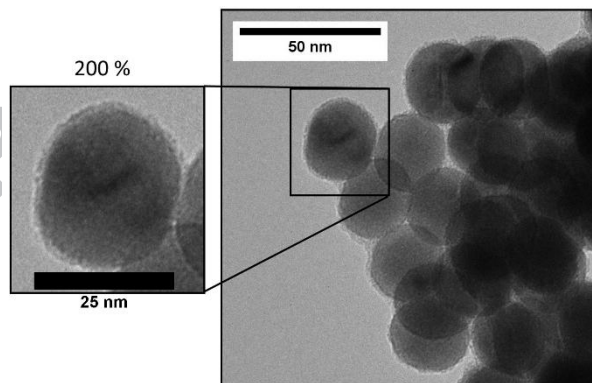


Figure 3. TEM image of the coated nanoparticles with 5.5 bilayers of (PAA/PAH) on the surface.

Scale bar is 50 nm and the inset zoom 200 % with a 25 nm scale bar.

### Crosslinking of the bilayers

The thermal crosslinking between the carboxyl group of PAA and amine group of PAH has been successfully demonstrated in the literature between 130-215 °C [30,33,35,36]. Due to low amount of sample material we chose to test the crosslinking by heating the nanomaterial (*ca.* 50 mg) for two hours at both 180 and 200 °C in N<sub>2</sub> atmosphere (Figure S5). This was done with material coated with five bilayers of PAA/PAH without the additional PAA on the surface to remove the effect of free carboxyl acid (-COOH) in the FT-IR spectra. From the FT-IR spectra it could be observed that crosslinking occurred at both temperatures but no clear difference between these two temperatures could be found. The damage to the surface modifications is expected due to the thermal analysis of the coated materials in which the mass drop is seen to increase already at the 200 °C. As the upconversion luminescence of the material crosslinked at 200 °C was weaker than that of 180 °C material (Figure S5) the latter was chosen as crosslinking temperature without further studies.

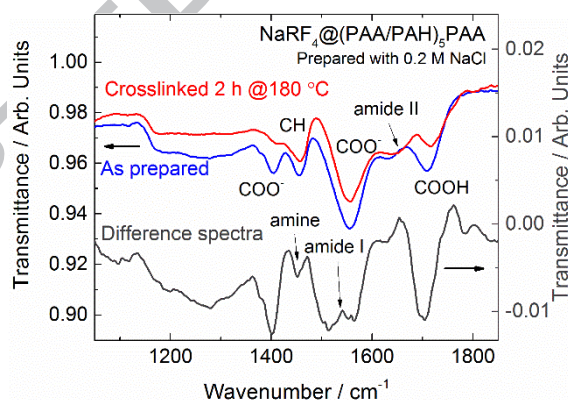


Figure 4. FT-IR spectra of the as-prepared and crosslinked coated nanomaterials prepared with ionic concentration of 0.2 M NaCl and their difference spectra.

When a difference FT-IR spectra is drawn from the 5.5 bilayer coated as-prepared and crosslinked nanomaterials it can be observed that the carboxyl and amine related vibrations

(1400, 1570, 1710 and 800  $\text{cm}^{-1}$ , respectively) are reduced and the amide related vibrations at *ca.* 1550 and 1660  $\text{cm}^{-1}$  are increasing suggesting that the crosslinking was successful (Figure 4) [30,33]. From the FT-IR spectra of the crosslinked nanomaterials it could be seen that there are still remaining  $\text{COO}^-$  vibrations from the final PAA layer on the surface as expected (Figure S6). After crosslinking, a change could be observed in the zeta potential at the first bilayer of the materials as it drops *ca.* 15 mV with both ionic concentrations in all materials (Figure 2, S4). This suggested that the crosslinking of the first bilayer removes the positive charge inside the polyelectrolyte multilayers. With the higher number of bilayers the change in zeta potential is not as big suggesting that even without the crosslinking the surface structure is more defined with the higher number of bilayers.

### Particle disintegration

The particle disintegration was monitored in aqueous environments using a fluoride selective electrode. We also studied the disintegration behavior in the presence of a low concentration of fluoride and in those measurements an external  $10^{-5}$  M of NaF was introduced into the aqueous solutions. The external fluoride concentration is expected to decelerate the disintegration process. Lahtinen et al. have previously studied the fluoride concentration effect on the disintegration of the nanoparticles up to 100 mM [15]. However, this concentration is already too high for the fluoride electrode response and thus unavailable for our measurement. The external fluoride was then subtracted from the data to obtain the actual release of the internal fluoride from the nanoparticles. From this data, a 1<sup>st</sup> order exponential fit was made to determine the total disintegration of the particle as the disintegration is expected to slow down as the equilibrium is reached with the fluoride concentration of the solution. However, it must be noted that in the

case of the coated nanoparticles this is expected to be more complicated because the concentration of the fluoride ions is expected to vary when different parts of the environments are considered (*e.g.* direct particle surface, the bilayer structure and the whole aqueous solution). For the fits the first 30 minutes were discarded since it takes 30 minutes for the instantly removed fluoride ions to reach the electrode through the dialysis barrier. The internal fluoride release rate during the measurement was estimated from the exponential fit derivative.

The used core materials released between 1.7-2.3 mol-% of fluoride ions during the 24 h measurement window. The differences in the disintegration are expected to arise from the size of the particles (the largest particle disintegrated the least) and from the possible differences in the remaining surface impurities within the core materials. The total extrapolated disintegration was from 2.7 to 3.4 mol-% for the core materials (Table S2). Using external fluoride the disintegration was decelerated slightly (*ca.* 1 mol-%). The behavior of the core particle is similar to the data obtained by Lisjak et al. where in the course of three days the fraction of fluoride dissolved in water was 3.7 mol-% [39]. However, they used higher concentration of UCNPs (1 mg/ml) which is expected to make the UCNPs disintegrate less than those made with lower UCNP concentration [15].

From the coated nanomaterials the 5.5 bilayers of PAA/PAH were the most successful in decelerating the fluoride release from the nanoparticle surface (Figure S7). In addition, already the first 1.5 bilayers were also successful but not as efficient. The biggest differences in the internal fluoride release were obtained from the higher number of coated bilayers. Crosslinking of the bilayers decelerated the disintegration even more during the measurement window, but in

some cases the overall extrapolated disintegration was similar to that of the as-prepared materials regardless of the crosslinking. The most efficient coatings in decelerating the disintegration were 5.5 bilayers prepared with ionic concentration of 0.2 M NaCl with or without the crosslinking.

The fluoride release rate curves showed that for these efficient coatings the release of the internal fluoride ions is decelerated faster than for the others (Figure 5, S8). However, the curves of the coated materials prepared with 0.1 M NaCl using additional 10 mM of NaF during the coating suggested that the release of the internal fluoride ions was the slowest with their crosslinked 5.5 bilayer material even though the overall release during the measurement window is slightly higher. This suggests that during the coating with additional fluoride some of the fluorides were accommodated by the positive amine sites of PAH creating a higher fluoride surface concentration within the formed bilayer structure and thus decelerating the release of the internal fluorides from the nanoparticle. Especially during the first five hours the difference between the fluoride release rates between the crosslinked and unlinked materials was significant. This suggests that the crosslinking can benefit specially the applications with short measurement windows.

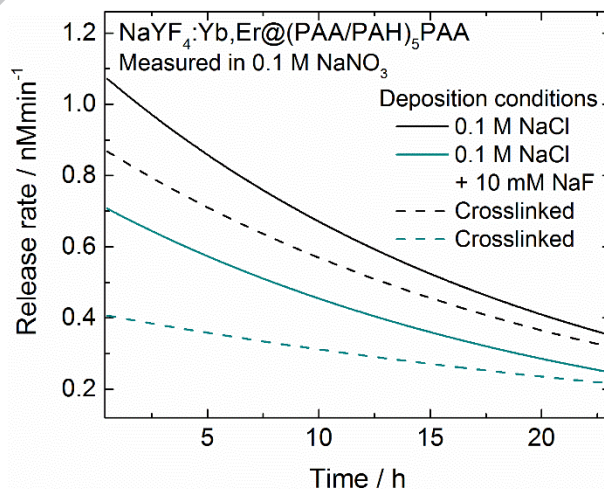


Figure 5. Fluoride release rate from the 5.5 bilayer coated nanomaterials made with 0.1 M NaCl measured in 0.1 M NaNO<sub>3</sub>.

Overall, the disintegration was slower from the coated nanomaterials prepared with additional fluoride present. We believe that when UCNPs are coated while there is additional fluoride present the rapid first hydrolysis of the fluorides on the particle surface [39] can be completely prevented during the coating process. This means that the disintegration has to start from an intact UCNP surface during the fluoride release measurement. As the surface is intact the process is slower. This means that without additional fluoride present during the coating the surface ions are already lost during the modification steps resulting in weakened surface properties.

The equilibrium state of the fluoride concentration in NaNO<sub>3</sub>(aq) is reached fastest (*ca.* 75 hours) with the materials coated with 5.5 bilayers of (PAA/PAH) using 0.2 M NaCl concentration regardless of the crosslinking (Figure S9). With the used cores and materials coated with 5.5 bilayers using the 0.1 M NaCl concentration the disintegration continued past the 75 hours and the equilibrium was reached only after 100 hours. The crosslinked materials had lower rate constants than did the non-crosslinked ones (Table S3) confirming that the internal fluoride release in them is slower than in those without crosslinking. However, no other trends could be observed with the coated materials.

Table 1. Disintegration of UCNPs coated with 5.5 bilayers with selected deposition conditions measured with 0.1 M NaNO<sub>3</sub>(aq) with or without external 10<sup>-5</sup> M NaF(aq) at 23 hours and in extrapolated equilibrium (200 h).

Deposition conditions with	x (F) @ 23 h / mol-%	x(F) @ 200 h / mol-%
----------------------------	-------------------------	-------------------------

5.5 bilayers	no fluoride	external fluoride	no fluoride	external fluoride
0.1 M NaCl	1.7	1.1	2.4	1.7
above crosslinked	1.4	0.5	2.2	1.6
0.1 M NaCl + 10mM NaF	1.3	1.5	1.9	1.9
above crosslinked	1.1	0.8	2.1	1.9
0.2 M NaCl	1.4	1.0	1.7	1.4
above crosslinked	1.3	0.8	1.8	1.3

When measurements from the materials having 5.5 bilayers on the nanoparticle surface were conducted in the presence of external  $10^{-5}$  M NaF in the nitrate solution it was observed that the internal fluoride release with the coated materials decreased (Table 1, Table S2, Figure S7). This is in agreement with the previously reported studies in which presence of 1 mM KF during the measurement prevented the particle disintegration [15]. However, it was interesting that with external fluoride present at the measurement with the nanomaterials coated with additional fluoride the release of the internal fluoride increased. It may be that this is due to such fluoride ions that have been captured within the coating layers during the coating process. Their release is seen as an apparent increase in the fluoride disintegration. This is expected to happen also with  $\text{NaNO}_3(\text{aq})$  and thus the observed released  $x(\text{F})$  for the as prepared materials made with the presence of external fluoride may be misleading. However, during the crosslinking some of this additional fluoride in the structure is expected to evaporate [37].

### Upconversion luminescence properties

All of the materials produced the desired visible upconversion luminescence from  $\text{Er}^{3+}$  ions in green ( ${}^2\text{H}_{11/2}$ ,  ${}^4\text{S}_{3/2} \rightarrow {}^4\text{I}_{15/2}$ ) and red ( ${}^4\text{F}_{9/2} \rightarrow {}^4\text{I}_{15/2}$ ) when excited at 973 nm ( $10\,280\text{ cm}^{-1}$ ). This is made possible through the energy transfer upconversion process from the excitation absorbing ytterbium sensitizer ions [40,41].

It could be observed that regardless of the layering conditions the first bilayer of the as prepared coating resulted in an increase of up-conversion emission intensity. Thus, this bilayer was the most efficient in shielding the upconversion luminescence obtained from the core as the coating does not have optically active components. After the first bilayer the upconversion luminescence decreased with increasing number of layers below the core materials' luminescence (Figure S10). Crosslinking of the as prepared coating resulted in further enhancement of the luminescence of the first bilayer but with the increasing number of bilayers with the ionic concentrations of 0.1 and 0.2 M NaCl prepared without additional fluoride the enhancement was lost. However, with the coating prepared at the presence of additional fluoride the upconversion luminescence enhanced also after crosslinking (Figure 6). This could indicate that the water in the bilayer structure could be responsible for the luminescence emission quenching with the increasing number of bilayers. The crosslinking of the bilayers can also increase compactness of the coating which can affect the absorption of the bilayers creating less interference with the emission. This confirmed that the first steps of disintegration of UCNPs have started during the surface modifications if they are made in aqueous environments without additional fluoride. The crosslinking of the coating does not enhance the obtained upconversion luminescence if the surface has already been covered with  $\text{OH}^-$  from the water molecules responsible for the quenching [13,42]. While the total luminescence intensity is decreasing through increasing amount of bilayers the red-to-green ratio of the materials is the lowest with the five bilayers of PAA/PAH suggesting that the layers are shielding especially the green upconversion luminescence from the  $\text{H}_2\text{O}$  molecules (Table S4) [21,40]. When the coating was prepared at the presence of additional fluoride the red-to-green ratio remained similar regardless of the number of coated bilayers. This also suggests that the core particle remains intact during the coating

procedure. However, further research and studies on the behavior of the upconversion luminescence with this type of coatings is still needed but the result obtained here seem promising.

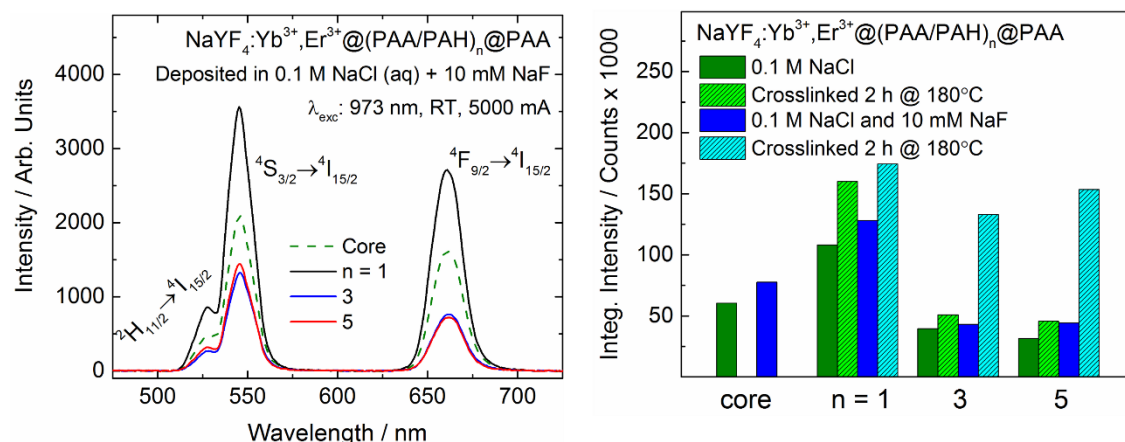


Figure 6. Upconversion luminescence of the coated and crosslinked UCNPs prepared with additional 10 mM NaF present at the coating (left) and integrated intensity of the upconversion luminescence with coatings prepared with or without additional fluoride (right).

## CONCLUSIONS

A successful layer-by-layer coating of upconverting nanoparticles with PAA/PAH polyelectrolyte multilayers is demonstrated with crosslinking the bilayer structure. Our research provides new information about the use of the layer-by-layer method in protecting the upconverting nanoparticles from environmental effects. It also simultaneously introduces surface modifications offering the possibility for further biomolecule conjugation. We observed that using additional fluoride during the coating procedure the upconversion luminescence of the NaYF<sub>4</sub>:Yb<sup>3+</sup>,Er<sup>3+</sup> core nanoparticles can be enhanced and maintained with increasing number of bilayers. Our research is in line with the previous observations that the disintegration is affected by the fluoride environment in aqueous solutions [15,39]. In contrast to the previous research,

where disintegration is strong in the beginning of the measurement, our surface modifications shield the nanoparticles from disintegration especially during the first five hours.

The bilayer formation was confirmed with various methods and it was successful regardless of the ionic concentration used during the coating. The crosslinking of the PAA and PAH bilayers was successful and could be observed from both FT-IR spectra as well as from the zeta potential measurements. Crosslinking of the bilayers created more defined coating structure on the nanoparticle surface as the interlocked water molecules were evaporated during the procedure. As expected, the additive fluoride during the coating procedure had no effect on the bilayer formation but it had an effect on the upconversion luminescence intensity of the prepared materials.

The coatings successfully decelerated the fluoride release and disintegration of the upconverting  $\text{NaYF}_4:\text{Yb}^{3+},\text{Er}^{3+}$  nanoparticles. Especially the crosslinked coating prepared with additional fluoride present had a slower fluoride release rate, suggesting that when the nanoparticle remains intact during the surface modifications the crosslinking of the bilayers decelerates the movement of fluoride ions into the aqueous solution. The decelerating effect of the crosslinking seems to be the most beneficial during the first five hours in water which makes it a good candidate for applications needing a short time shielding. In addition, all of the coatings are able to reduce the disintegration of the particles when immersed in aqueous solution compared with the disintegration of the non-coated nanoparticles.

Further research and focus are needed for the applicability of these surface modifications but the results presented here are promising. This invites new possibilities for further exploiting the various properties of the layer-by-layer method and the bilayer formation in the shielding of upconverting nanoparticles.

## SUPPLEMENTARY INFORMATION

Additional characterization data for materials (FT-IR spectra, thermal analysis, zeta potential, fluoride release data, and upconversion luminescence spectra with red-to-green ratios) are available in the supporting information.

## ACKNOWLEDGEMENT

Financial support to EP from Turku University foundation and the Vilho, Yrjö and Kalle Väisälä Foundation is gratefully acknowledged. Ermei Mäkilä is thanked for the help during the zeta potential measurements. Markus Peurla is thanked for the TEM images. This work made use of the Laboratory of Electron Microscopy premises at University of Turku.

## REFERENCES

- [1] Z. Farka, T. Juřík, D. Kovář, L. Trnková, P. Skládal, Nanoparticle-Based Immunochemical Biosensors and Assays : Recent Advances and Challenges, *Chem. Rev.* 117 (2017) 9973–10042.
- [2] R. Arppe, L. Mattsson, K. Korpi, S. Blom, Q. Wang, T. Riuttamäki, et al., Homogeneous Assay for Whole Blood Folate Using Photon Upconversion, *Anal. Chem.* 87 (2015) 1782–1788.
- [3] M. Ylihärsilä, E. Harju, R. Arppe, L. Hattara, J. Hölsä, P. Saviranta, et al., Genotyping of clinically relevant human adenoviruses by array-in-well hybridization assay, *Clin. Microbiol. Infect.* 19 (2013) 551–557.
- [4] G. Chen, H. Qiu, P.N. Prasad, X. Chen, Upconversion Nanoparticles: Design,

- Nanochemistry, and Applications in Theranostics, *Chem. Rev.* 114 (2014) 5161–5214.
- [5] F. Auzel, Upconversion and Anti-Stokes Processes with f and d Ions in Solids, *Chem. Rev.* 104 (2004) 139–173.
- [6] J. Zhou, Q. Liu, W. Feng, Y. Sun, F. Li, Upconversion Luminescent Materials : Advances and Applications, *Chem. Rev.* 115 (2015) 395–465.
- [7] H.H. Gorris, U. Resch-Genger, Perspectives and challenges of photon-upconversion nanoparticles - Part II bioanalytical applications, *Anal. Bioanal. Chem.* 409 (2017) 5875–5890.
- [8] T. Rinkel, A.N. Raj, S. Dühnen, M. Haase, Synthesis of 10 nm  $\beta$ -NaYF<sub>4</sub>:Yb,Er/NaYF<sub>4</sub> Core / Shell Upconversion Nanocrystals with 5 nm Particle Cores, *Angew. Chemie - Int. Ed.* 55 (2016) 1164–1167.
- [9] Y. Li, Y. Dong, T. Aidilibike, X. Liu, J. Guo, W. Qin, Growth phase diagram and upconversion luminescence properties of NaLuF<sub>4</sub>:Yb<sup>3+</sup>/Tm<sup>3+</sup>/Gd<sup>3+</sup> nanocrystals, *RSC Adv.* 7 (2017) 44531–44536.
- [10] K.W. Krämer, D. Biner, G. Frei, H.U. Güdel, M.P. Hehlen, S.R. Lüthi, et al., Hexagonal Sodium Yttrium Fluoride Based Green and Blue Emitting Upconversion Phosphors, *Chem. Mater.* 16 (2004) 1244–1251.
- [11] J.L. Sommerdijk, On the Excitation Mechanisms of the Infrared-Excited Visible Luminescence in Yb<sup>3+</sup>, Er<sup>3+</sup>-doped Fluorides, *J. Lumin.* 4 (1971) 441–449.
- [12] Y. Hossan, A. Hor, Q. Luu, S.J. Smith, P.S. May, M.T. Berry, Explaining the Nanoscale Effect in the Upconversion Dynamics of  $\beta$ -NaYF<sub>4</sub>:Yb<sup>3+</sup>, Er<sup>3+</sup> Core and Core–Shell Nanocrystals, *J. Phys. Chem. C.* 121 (2017) 16592–16606.
- [13] R. Arppe, I. Hyppänen, N. Perälä, R. Peltomaa, M. Kaiser, C. Würth, et al., Quenching of

- the upconversion luminescence of  $\text{NaYF}_4:\text{Yb}^{3+},\text{Er}^{3+}$  and  $\text{NaYF}_4:\text{Yb}^{3+},\text{Tm}^{3+}$  nanophosphors by water: the role of the sensitizer  $\text{Yb}^{3+}$  in non-radiative relaxation., *Nanoscale*. 7 (2015) 11746–11757.
- [14] N.J.J. Johnson, S. He, S. Diao, E.M. Chan, H. Dai, A. Almutairi, Direct Evidence for Coupled Surface and Concentration Quenching Dynamics in Lanthanide-doped Nanocrystals, *J. Am. Chem. Soc.* 139 (2017) 3275–3282.
- [15] S. Lahtinen, A. Lyytikäinen, H. Päckilä, E. Hömppi, N. Perälä, M. Lastusaari, et al., Disintegration of Hexagonal  $\text{NaYF}_4:\text{Yb}^{3+},\text{Er}^{3+}$  Upconverting Nanoparticles in Aqueous Media: The Role of Fluoride in Solubility Equilibrium, *J. Phys. Chem. C*. 121 (2017) 656–665.
- [16] O. Plohl, M. Kraft, J. Kovac, B. Belec, M. Ponikvar-Svet, C. Würth, et al., Optically Detected Degradation of  $\text{NaYF}_4:\text{Yb},\text{Tm}$ -based Upconversion Nanoparticles in Phosphate Buffered Saline Solution, *Langmuir*. 33 (2017) 553–560.
- [17] Y. Wang, L. Tu, J. Zhao, Y. Sun, X. Kong, H. Zhang, Upconversion Luminescence of  $\beta\text{-NaYF}_4:\text{Yb}^{3+},\text{Er}^{3+}$ @ $\beta\text{-NaYF}_4$  Core/Shell Nanoparticles: Excitation Power Density and Surface Dependence, *J. Phys. Chem. C*. 113 (2009) 7164–7169.
- [18] K. Prorok, A. Bednarkiewicz, Energy Migration Up-conversion of  $\text{Tb}^{3+}$  in  $\text{Yb}^{3+}$  and  $\text{Nd}^{3+}$  Codoped Active-Core/Active-Shell Colloidal Nanoparticles, *Chem. Mater.* 28 (2016) 2295–2300.
- [19] Z. Li, L. Wang, Z. Wang, X. Liu, Y. Xiong, Modification of  $\text{NaYF}_4:\text{Yb},\text{Er}@ \text{SiO}_2$  Nanoparticles with Gold Nanocrystals for Tunable Green-to-Red Upconversion Emissions, *J. Phys. Chem. C*. 115 (2011) 3291–3296.
- [20] X. Chen, D. Zhou, W. Xu, J. Zhu, G. Pan, Z. Yin, et al., Fabrication of Au-Ag

- nanocage@NaYF<sub>4</sub>@NaYF<sub>4</sub>:Yb,Er Core- Shell Hybrid and its Tunable Upconversion Enhancement, *Sci. Rep.* 7 (2017) 41079.
- [21] S. Wilhelm, M. Kaiser, C. Würth, J. Heiland, C. Carrillo-Carrion, V. Muhr, et al., Water dispersible upconverting nanoparticles: effects of surface modification on their luminescence and colloidal stability, *Nanoscale.* 7 (2015) 1403–1410.
- [22] A. Sedlmeier, H.H. Gorris, Surface modification and characterization of photon-upconverting nanoparticles for bioanalytical applications, *Chem. Soc. Rev.* 44 (2014) 1526–1560.
- [23] O. Plohl, S. Kralj, B. Majaron, E. Fröhlich, M. Ponikvar-svet, D. Makovec, et al., Amphiphilic coatings for the protection of upconverting nanoparticles against dissolution in aqueous media, *Dalt. Trans.* 46 (2017) 6975–6984.
- [24] E. Palo, S. Lahtinen, H. Päckilä, M. Salomäki, T. Soukka, M. Lastusaari, Effective Shielding of NaYF<sub>4</sub>:Yb<sup>3+</sup>,Er<sup>3+</sup> Upconverting Nanoparticles in Aqueous Environments Using Layer-by-Layer Assembly, *Langmuir.* 34 (2018) 7759–7766.
- [25] G. Decher, Fuzzy Nanoassemblies: Toward Layered Polymeric Multicomposites, *Science* 277 (1997) 1232–1237.
- [26] M.M. De Villiers, D.P. Otto, S.J. Strydom, Y.M. Lvov, Introduction to nanocoatings produced by layer-by-layer (LbL) self-assembly, *Adv. Drug Deliv. Rev.* 63 (2011) 701–715.
- [27] X. Hong, J. Li, M. Wang, J. Xu, W. Guo, J. Li, et al., Fabrication of magnetic luminescent nanocomposites by a layer-by-layer self-assembly approach, *Chem. Mater.* 16 (2004) 4022–4027.
- [28] G. Schneider, G. Decher, Functional core/shell nanoparticles via layer-by-layer assembly.

- Investigation of the experimental parameters for controlling particle aggregation and for enhancing dispersion stability, *Langmuir*. 24 (2008) 1778–1789.
- [29] E. Palo, M. Salomäki, M. Lastusaari, Surface modification of upconverting nanoparticles by layer-by-layer assembled polyelectrolytes and metal ions, *J. Colloid Interface Sci.* 508 (2017) 137–144.
- [30] A.M. Balachandra, J. Dai, M.L. Bruening, Enhancing the Anion-Transport Selectivity of Multilayer Polyelectrolyte Membranes by Templating with  $\text{Cu}^{2+}$ , *Macromolecules*. 35 (2002) 3171–3178.
- [31] E. Palo, M. Tuomisto, I. Hyppänen, H.C. Swart, J. Hölsä, T. Soukka, et al., Highly Uniform Up-Converting Nanoparticles: Why You Should Control Your Synthesis Even More, *J. Lumin.* 185 (2017) 125–131.
- [32] N. Bogdan, F. Vetrone, G.A. Ozin, J.A. Capobianco, Synthesis of ligand-free colloiddally stable water dispersible brightly luminescent lanthanide-doped upconverting nanoparticles, *Nano Lett.* 11 (2011) 835–840.
- [33] J.J. Harris, P.M. Derosé, M.L. Bruening, Synthesis of Passivating, Nylon-Like Coatings through Cross-Linking of Ultrathin Polyelectrolyte Films, *J. Am. Chem. Soc.* 121 (1999) 1978–1979.
- [34] M.F. Elahi, G. Guan, L. Wang, M.W. King, Influence of Layer-by-Layer Polyelectrolyte Deposition and EDC/NHS Activated Heparin Immobilization onto Silk Fibroin Fabric, *Materials (Basel)*. 7 (2014) 2956–2977.
- [35] Y. Guo, W. Geng, J. Sun, Layer-by-Layer Deposition of Polyelectrolyte-Polyelectrolyte Complexes for Multilayer Film Fabrication, *Langmuir*. 25 (2009) 1004–1010.
- [36] Y. Ma, J. Sun, J. Shen, Ion-Triggered Exfoliation of Layer-by-Layer Assembled

- Poly(acrylic acid)/Poly(allylamine hydrochloride) Films from Substrates: A Facile Way To Prepare Free-Standing Multilayer Films, *Chem. Mater.* 19 (2007) 5058–5062.
- [37] E. Harju, I. Hyppänen, J. Hölsä, J. Kankare, M. Lahtinen, M. Lastusaari, et al., Polymorphism of  $\text{NaYF}_4:\text{Yb}^{3+},\text{Er}^{3+}$  up-conversion luminescence materials, *Z. Krist. Proc.* 1 (2011) 381–387.
- [38] P. Chodanowski, S. Stoll, Polyelectrolyte Adsorption on Charged Particles in the Debye-Hueckel Approximation. A Monte Carlo Approach, *Macromolecules.* 34 (2001) 2320–2328.
- [39] D. Lisjak, O. Plohl, J. Vidmar, B. Majaron, M. Ponikvar-svet, Dissolution Mechanism of Upconverting  $\text{AYF}_4:\text{Yb},\text{Tm}$  (A = Na or K) Nanoparticles in Aqueous Media, *Langmuir.* 32 (2016) 8222–8229.
- [40] I. Hyppänen, N. Höysniemi, R. Arppe, M. Schäferling, T. Soukka, Environmental Impact on the Excitation Path of the Red Upconversion Emission of Nanocrystalline  $\text{NaYF}_4:\text{Yb}^{3+},\text{Er}^{3+}$ , *J. Phys. Chem. C.* 121 (2017) 6924–6929.
- [41] M.T. Berry, P.S. May, Disputed Mechanism for NIR-to-Red Upconversion Luminescence in  $\text{NaYF}_4:\text{Yb}^{3+},\text{Er}^{3+}$ , *J. Phys. Chem. A.* 119 (2015) 9805–9811.
- [42] F.T. Rabouw, P.T. Prins, P. Villanueva-delgado, M. Castelijns, R.G. Geitenbeek, A. Meijerink, Quenching Pathways in  $\text{NaYF}_4:\text{Er}^{3+},\text{Yb}^{3+}$  Upconversion Nanocrystals, *ACS Nano.* 12 (2018) 4812–4823.

## GRAPHICAL ABSTRACT

